

1 Plant Physiology

2 **Host-induced gene silencing of the MAPKK gene *PsFUZ7***

3 **confers stable resistance to wheat stripe rust**

4 **Xiaoguo Zhu¹, Tuo Qi¹, Qian Yang¹, Fuxin He¹, Chenglong Tan¹, Wei Ma¹,**

5 **Ralf Thomas Voegelé², Zhensheng Kang^{*1}, and Jun Guo^{*1}**

6 ¹ State Key Laboratory of Crop Stress Biology for Arid Areas, College of Plant
7 Protection, Northwest A&F University, Yangling 712100, Shaanxi, China.

8 ² Department of Phytopathology, Institute of Phytomedicine, Faculty of
9 Agricultural Sciences, University of Hohenheim, 70599 Stuttgart, Germany

10 * Authors for correspondence:

11 Jun Guo: Northwest A&F University, E-mail: guojunwgq@nwsuaf.edu.cn;

12 Tel/fax: 0086-29-87082439.

13 Zhensheng Kang: Northwest A&F University, E-mail:

14 kangzs@nwsuaf.edu.cn; Tel/fax: 0086-29-87080061

15 **Running title:** HIGS of *PsFUZ7* confers stable resistance to *Pst*.

16 **One sentence summary:** Transgenic wheat expressing a double-stranded RNA
17 targeting MAPKK gene *PsFUZ7* from *Puccinia striiformis* f. sp. *tritici* exhibits strong
18 resistance to stripe rust.

19 **List of authors' contributions**

20 J.G. and Z.S.K designed the experiments; X.G.Z., T.Q., Q.Y., F.X.H., C.L.T and

21 W.M. performed the experiments; X.G.Z., J.G., R.T.V, and Z.S.K analyzed the
22 data and wrote the paper. All authors discussed the results and commented on
23 the manuscript.

24 **Funding information**

25 This study was supported by the National Natural Science Foundation of China
26 (No. 31620103913), the National Basic Research Program of China (No.
27 2013CB127700), the 111 Project from the Ministry of Education of China (No.
28 B07049) and Natural Science Basic Research Plan in Shaanxi Province of
29 China (2017JM3007).

30 **ABSTRACT**

31 RNA interference (RNAi) is a powerful genetic tool to accelerate research in
32 plant biotechnology and to control biotic stresses by manipulating target gene
33 expression. However, the potential of RNAi in wheat to efficiently and durably
34 control the devastating stripe rust fungus *Puccinia striiformis* f. sp. *tritici* (*Pst*),
35 remained largely under explored, so far. To address this issue, we generated
36 transgenic wheat lines expressing double-stranded RNA targeting *PsFUZ7*
37 transcripts of *Pst*. We analyzed expression of *PsFUZ7* and related genes, and
38 resistance traits of the transgenic wheat lines. We show that *PsFUZ7* is an
39 important pathogenicity factor which regulates infection and development of
40 *Pst*. A *PsFUZ7* RNAi construct stably expressed in two independent transgenic
41 wheat lines confers strong resistance to *Pst*. *Pst* hyphal development is
42 strongly restricted, and necrosis of plant cells in resistance responses was
43 significantly induced. We conclude that trafficking of RNA molecules from
44 wheat plants to *Pst* may lead to a complex molecular dialogue between wheat
45 and the rust pathogen. Moreover, we confirm the RNAi-based crop protection
46 approaches can be used as a novel control strategy against rust pathogens in
47 wheat.

48 **INTRODUCTION**

49 Global wheat yields are estimated to be reduced by 3% to over 90% per
50 year because of the obligate biotrophic pathogen *P. striiformis* f. sp. *tritici* (*Pst*),
51 jeopardizing global food security (Wellings, 2011; Chen, 2014). It is evident
52 that *Pst* constitutes a significant threat to wheat production worldwide.
53 Currently, approaches to manage this disease rely on cultivar resistance
54 coupled with fungicide application (Chen, 2014). However, driven by a greater
55 need for wheat production (Singh et al., 2011), the necessity for environmental
56 protection (Ishii, 2006), the constant evolution of virulence in rust fungi (Chen
57 et al., 2009), and the loss of natural resistance in wheat cultivars (McIntosh et
58 al., 1995), innovative alternative approaches to control rust disease are
59 urgently required. To date, several technologies have been used to transiently
60 silence *Pst* genes to restrict pathogen development (Panwar et al., 2013; Fu et
61 al., 2014). However, the pathogen is capable of overcoming this transient
62 resistance barrier, and hence, strategies conferring durable resistance to *Pst*
63 must be sought.

64 A powerful genetic tool, RNA interference (RNAi), a conserved eukaryotic
65 mechanism that performs a crucial role in gene regulation, has been used to
66 enhance crop resistance by silencing critical genes (Bartel, 2004; Baulcombe,
67 2004). A key conserved trait of RNAi is the cleavage of precursor double
68 stranded RNA (dsRNA) into short 21-24 nucleotide small interfering RNAs
69 (siRNAs) by a ribonuclease called DICER, or Dicer-like (DCL) (Fagard et al.,
70 2000). siRNAs are then incorporated into the RNA-induced silencing complex
71 (RISC) containing an Argonaute (AGO) protein (Fagard et al., 2000).
72 Subsequently, specific degradation of the target mRNA sharing sequence
73 similarity with the inducing dsRNA takes place (Ghildiyal and Zamore, 2009;
74 Liu, 2010). Numerous reports have demonstrated the efficiency of RNAi to
75 improve control of bacteria, viruses, fungi, insects, nematodes, and parasitic
76 weeds (Saurabh et al., 2014). Insects feeding on transgenic plants carrying
77 RNAi constructs against genes of the pest were severely constrained in their

78 development (Huang et al., 2006; Baum et al., 2007; Mao et al., 2007). In
79 genetically engineered RNAi crop plants, defense against fungi was
80 substantially enhanced (Nowara et al., 2010; Koch et al., 2013; Ghag et al.,
81 2014). Host-Induced Gene Silencing (HIGS) of the *Fusarium* cytochrome P450
82 lanosterol C-14 α -demethylase (*CYP51*) gene, which is essential for ergosterol
83 biosynthesis, confers resistance of barley to *Fusarium* species (Koch et al.,
84 2013). During interaction of the host with the pathogen *Blumeria graminis*,
85 siRNA molecules are exchanged and restrict fungal development in plants
86 carrying RNAi constructs targeting fungal transcripts (Nowara et al., 2010).

87 Mitogen-activated protein kinase (MAPK) cascades regulate a variety of
88 cellular processes in response to extracellular and intracellular stimuli (Van
89 Drogen and Peter, 2002). In our study, the MAPK kinase gene *PsFUZ7*, which
90 was shown to play an important role in *Pst* virulence by regulating hyphal
91 morphology and development, was selected as target for RNAi. Our results
92 indicate that the expression of RNAi constructs in transgenic wheat plants
93 confers strong and durable resistance to *Pst*, along with a severe restriction of
94 *Pst* development. This efficient inhibition of disease development suggests
95 that HIGS is a powerful strategy to engineer transgenic wheat resistant against
96 the obligate biotrophic pathogen *Pst* and has potential as an alternative
97 approach to conventional breeding, or chemical treatment for the development
98 of environmentally friendly and durable resistance in wheat and other food
99 crops.

100

101

102 **RESULTS**

103 **Three MAPK Cascade Genes are Highly Induced during *Pst***
104 **Differentiation**

105 During our search for potential genes that regulate the development of *Pst*,
106 we identified and cloned five candidate genes from the virulent *Pst* strain
107 CYR32. These genes were found to be orthologs of *Ustilago maydis* MAPK
108 signaling pathway-related genes (Supplemental Table S1). Transcript profiles
109 assayed by quantitative real-time PCR (qRT-PCR) show that *PsKPP4*,
110 *PsFUZ7*, *PsKPP6*, and *PsCRK1* are all induced at early differentiation stages,
111 whereas *PsKPP2* is significantly down-regulated during this phase (Fig. 1).
112 Transcript levels of *PsKPP4*, *PsFUZ7*, and *PsKPP6* are increased more than
113 30-fold during the very early stage of colonization of wheat by urediospores
114 (12 h), and the time of primary haustorium formation (18 h), the stage
115 indicating successful colonization of the host. *PsKPP4* and *PsFUZ7* are
116 induced more than 20-fold during secondary hyphae formation (48-72 h), the
117 stage essential for hyphal expansion. These results suggest that *PsKPP4*,
118 *PsFUZ7*, and *PsKPP6* participate in early *Pst* development. Therefore, these
119 genes were chosen as target genes for subsequent virus-induced gene
120 silencing (VIGS) experiments.

121 **Transient Silencing of *PsFUZ7* Significantly Inhibits Growth of *Pst***

122 VIGS mediated by the barley stripe mosaic virus (BSMV) has been
123 established in barley and wheat (Holzberg et al., 2002; Scofield et al., 2005).
124 To confirm the effect of silencing *PsKPP4*, *PsFUZ7*, and *PsKPP6* during the
125 interaction between wheat and *Pst* strain CYR32, two ~250-bp silencing
126 sequences of each gene were derived from the 5'- and the 3'-prime end of the
127 gene to generate different BSMV constructs (Supplemental Table S2),
128 respectively. At 14 days post inoculation (dpi) with *Pst*, generation of uredia is
129 suppressed in plants inoculated with BSMV-silencing sequences, and those
130 carrying BSMV:*PsFUZ7*-as constructs show the highest inhibition of uredia

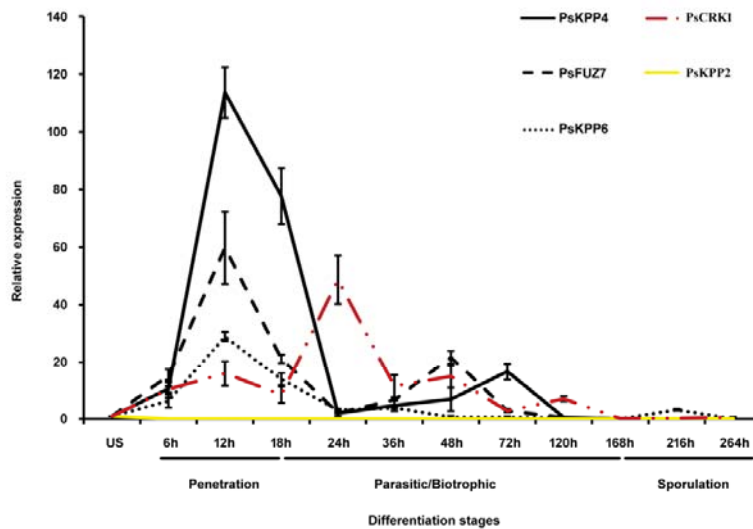


Figure 1. Transcript profiles of five MAPK cascade genes at different *Pst* infection stages. Wheat leaves (Su11) were inoculated with fresh urediospores (CYR32) and kept in the dark and under high humidity for 24 h. Inoculated leaves were sampled at different time points according to the differentiation stage of *Pst*. Gene expression levels were normalized to the expression level of *PsEF-1*. Results are expressed as means \pm standard errors of three biological replicates. US: urediospores; 6 - 264 h: 6 - 264 hpi with CYR32. *PsKPP4*, MAP kinase kinase kinase gene; *PsFUZ7*: MAP kinase kinase gene; *PsKPP2*, *PsKPP6* and *PsCRK1*: MAP kinase genes.

131 formation (Fig. 2A). qRT-PCR analysis of total RNA isolated from silenced
 132 leaves sampled at 2 and 7 dpi, revealed effective reductions in transcript levels
 133 of the fungal target genes (Fig. 2B). Values are expressed relative to the
 134 endogenous *Pst* reference gene *EF-1* (*PsEF-1*), with the empty vector
 135 (BSMV: γ) set to 1 (Yin et al., 2011). To demonstrate the specificity of VIGS
 136 against *PsKPP4*, *PsFUZ7* and *PsKPP6*, the expression of their closest
 137 homologs at 2 dpi was also examined (Supplemental Fig. S1 and
 138 Supplemental Table S3).

139 Microscopic analyses revealed that initial haustorium formation and
 140 elongation of secondary hyphae are both reduced in BMSV:*PsFUZ7-1as* and

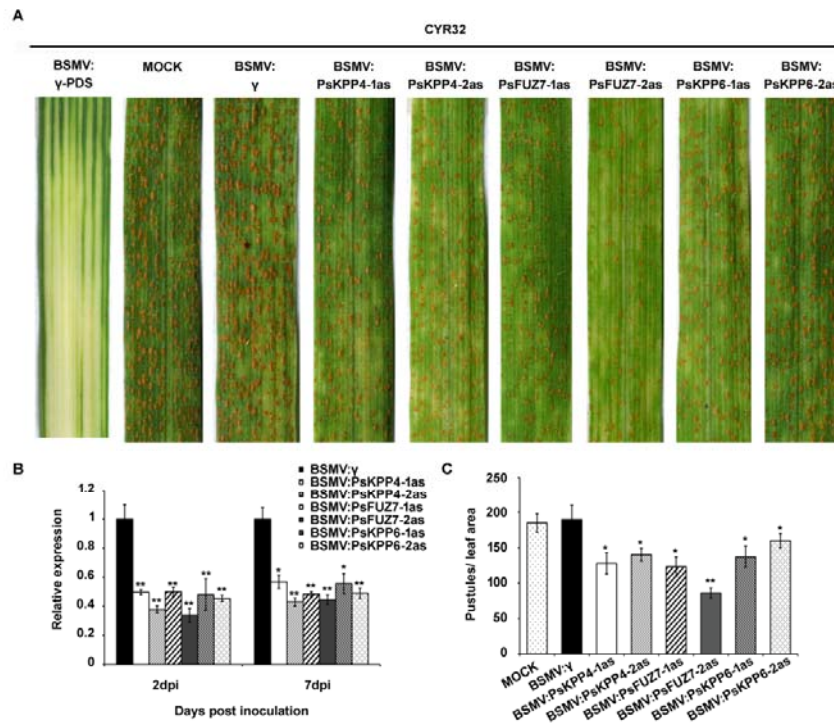


Figure 2. Functional assessment of *PsKPP4*, *PsFUZ7* and *PsKPP6* in the wheat–*Pst* interaction by virus-induced gene silencing. A, Phenotypes of fourth leaves inoculated with CYR32 at 14 dpi. Plants were pre-inoculated with FES buffer (mock), BSMV: *TaPDS*, BSMV: γ , BSMV: *PsKPP4*-1as, BSMV: *PsKPP4*-2as, BSMV: *PsFUZ7*-1as, BSMV: *PsFUZ7*-2as, BSMV: *PsKPP6*-1as, or BSMV: *PsKPP6*-2as, respectively. B, Relative transcript levels of *PsKPP4*, *PsFUZ7* and *PsKPP6* in knockdown plants inoculated with CYR32 at 2 and 7 dpi. Wheat leaves inoculated with BSMV: γ and sampled after inoculation with CYR32 were used as controls. Data were normalized to the transcript level of *PsEF-1*. Asterisks indicate $P < 0.05$, double asterisks indicate $P < 0.01$. C, Quantification of uredial density in silenced plants 14 dpi with CYR32. Differences were assessed using Student's t-tests. Values represent the means \pm standard errors of three independent samples. Asterisks indicate $P < 0.05$, double asterisks indicate $P < 0.01$.

141 BSMV: *PsFUZ7*-2as treated plants (Fig. 3). *PsFUZ7*-2as-silenced plants exhibit
 142 a more pronounced inhibition of haustorium formation and mycelial extension
 143 with decreased hyphal length and reduced size of infection areas than other
 144 silencing constructs. As a result, fewer uredia were produced in plants carrying
 145 BSMV: *PsFUZ7*-2as (Fig. 2C). This result indicates that *PsFUZ7* plays an
 146 important role in mycelial growth and development which eventually leads to a
 147 significant inhibition of uredia generation and virulence of *Pst*.

148 The Function of *PsFUZ7* is Conserved among Phytopathogenic Fungi

149 *PsFUZ7* contains the typical domain structure of MAPKKs, including 12

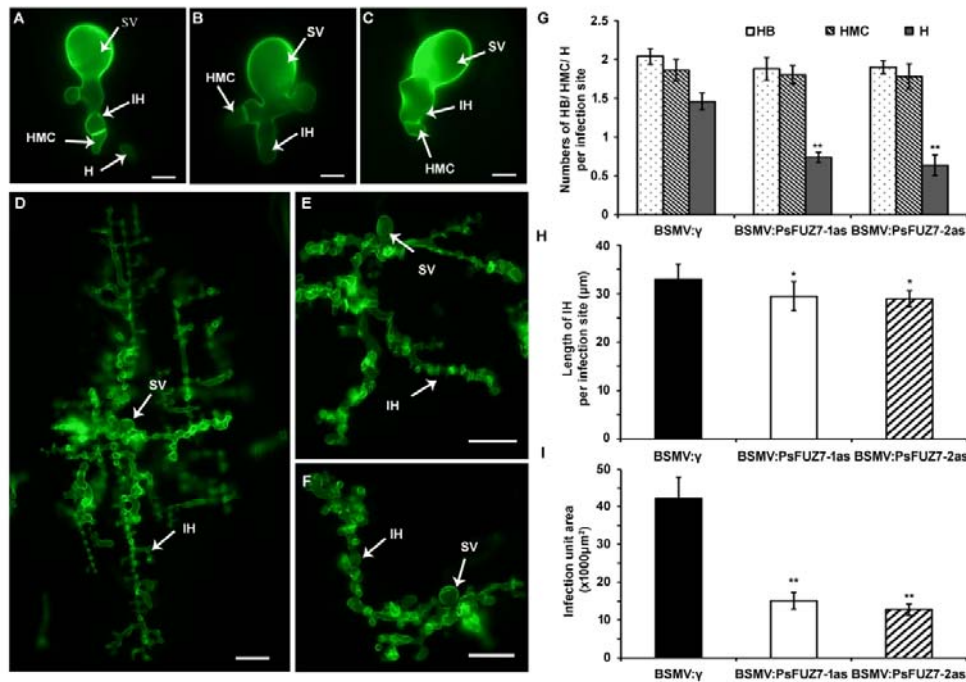


Figure 3. Epifluorescence observation of fungal growth in wheat inoculated with BSMV and infected with CYR32. Leaves inoculated with CYR32 were sampled at 48 and 120 hpi and examined under an epifluorescence microscope after staining with wheat germ agglutinin conjugated to Alexa-488 (Invitrogen, Carlsbad, CA, USA). Treatments include A, BSMV:γ; B, BSMV:PsFUZ7-1as and C, BSMV:PsFUZ7-2as inoculated with CYR32 at 48 hpi (Bars = 10 μm); D, BSMV:γ; E, BSMV:PsFUZ7-1as and F, BSMV:PsFUZ7-2as inoculated with CYR32 at 120 hpi (Bars = 50 μm). SV, substomatal vesicle; HMC, haustorial mother cell; IH, infection hypha; H, haustorium. G, Average number of haustoria (H), hyphal branches (HB) and haustorial mother cells (HMC) in wheat inoculated with BSMV constructs and infected with CYR32 at 48 hpi. H, Average length of infection hyphae (IH) measured from their origin at the substomatal vesicle to the tip of the hypha in wheat inoculated with BSMV constructs and infected with CYR32 at 48 hpi. I, Infection area per infection site in wheat inoculated with BSMV and infected with CYR32 at 120 hpi. Differences in G-I were assessed using Student's t-tests. Values represent the means ± standard errors of three independent samples. Asterisks indicate P < 0.05, double asterisks indicate P < 0.01.

150 catalytic kinase subdomains (Hamal et al., 1999), two putative phosphorylation
 151 sites, an activation loop (S/TXXXS/T) as the putative target of an upstream
 152 MAPKKK, and a DEJL motif (K/R-K/R-K/R-X (1-5)-L/I-X-L/I) at the N-terminus,
 153 which is known to function as a MAPK docking site (Supplemental Fig. S2)
 154 (Chen et al., 2012). Sequence alignments indicate that *PsFUZ7* shares 70 %,
 155 82 %, and 84 % sequence identity with orthologs from *Magnaporthe oryzae*, *P.*
 156 *triticina*, and *P. graminis* f. sp. *tritici*, respectively. Consistent with this high
 157 similarity, *PsFUZ7* partially complements the *Magnaporthe oryzae mst7*
 158 mutant in appressorium formation and plant infection (Supplemental Fig. S3).
 159 Overexpression of *PsFUZ7* in fission yeast results in morphological changes

160 and an increased sensitivity to environmental stresses (Supplemental Fig. S4).
161 In accordance with these *in vivo* data, *in vitro* assays revealed that stripe rust
162 urediospores treated with the kinase inhibitor U0126 germinate at a lower rate
163 and produce a higher frequency of abnormally differentiated and clearly
164 distorted germ tubes or spherical structures along the mycelial apex at 3 h and
165 6 h post-treatment (Supplemental Fig. S5). Overall, these results strengthen
166 the view that *PsFUZ7* may have important roles in pathogenesis.

167 **RNAi Constructs in Transgenic Wheat Plants Detected by Southern Blot** 168 **and PCR**

169 To test whether the stable expression of *PsFUZ7* silencing constructs can
170 confer resistance to *Pst*, the selected, most effective RNAi construct, a 759-bp
171 cassette containing an inverted repeat derived from *PsFUZ7-2as* was
172 introduced into vector pAHC25, and transformed into *Triticum aestivum* L. cv.
173 Xinong1376 (XN1376) by particle bombardment (Supplemental Fig. S6A). The
174 *PsFUZ7*-RNAi construct in transgenic wheat plants was detected by PCR
175 (Supplemental Fig. S6B), and the stable integration of RNAi constructs into the
176 wheat genome was verified by Southern blot with specific probes
177 (Supplemental Fig. S6C). No consecutive 21-24 nucleotide (nt) sequences
178 were found in wheat and/or other plant or fungal species for *PsFUZ7*
179 (Supplemental Table S4). To identify potential off-target sites, BLASTN was
180 performed using the target sequence. Among all putative off-targets examined,
181 12 sequences were detected in wheat and *Pst* at one or more locus with a 1-3
182 bp mismatch, respectively (Supplemental Fig. S7 and S8; Supplemental Table
183 S2). As shown in Supplemental Fig. S7 and S8, no significant down-regulation
184 was found in the potential putative off-target genes. Transgenic wheat lines
185 that contained RNAi constructs, displayed normal morphology, and set viable
186 seeds were assayed for resistance against *Pst*.

187 **Two T₃ Transgenic Wheat Lines Confer Strong Resistance to *Pst***

188 Two independent transgenic lines, L65 and L91, which were highly effective
189 in restricting the spread of *Pst*, were selected in T₃ generations and examined
190 at 16 dpi (Fig. 4A). To verify whether this phenotype is caused by the
191 expression and processing of siRNA, Northern blot analysis was performed
192 with RNA extracted from 14-day-old seedlings of the T₃ transgenic lines, using
193 the same specific probes as those used for Southern blot analyses. As shown
194 in Fig. 4B, a single band with the expected size of ~21 nt is present in
195 transgenic lines L65 and L91, while no signal can be detected in control plants,
196 documenting the presence of *PsFUZ7* siRNAs in the transgenic lines. To
197 further confirm that the expression of siRNA in wheat is able to silence
198 *PsFUZ7*, qRT-PCR was performed to analyze transcript abundance of
199 *PsFUZ7* in *Pst*-infected transgenic lines at 3, 10, 16 dpi. *PsFUZ7* transcripts in
200 L65 were reduced by 42.2 %, 48.3 %, and 49.3 % compared to control lines at
201 3, 10, 16 dpi, respectively. Similarly, *PsFUZ7* transcripts were reduced by
202 41.7 %, 69.9 % and 74.8 % in L91 (Fig. 4C). According to the McNeal's
203 uniform scale system (McNeal et al., 1971) the host response class of
204 transgenic lines L65 and L91 ranged from 1 to 3, indicating high or medium
205 resistance to *Pst*. By contrast, the response of control lines was in the 6 to 7
206 class, which along with abundant sporulation and little necrotic/chlorotic stripes
207 indicates susceptibility to *Pst* (Fig. 4D). Biomass analyses showed that both
208 transgenic lines exhibit significant reductions in fungal biomass ($P < 0.01$) of
209 68-71 % and 50-57 %, respectively, at 16 dpi with *Pst* (Fig. 4E). In addition,
210 compared with control plants, transcript levels of some MAPK signal
211 pathway-related genes (Fig. 5A), are reduced in *Pst*-infected transgenic lines
212 L65 and L91, while some plant defense-related genes are up-regulated (Fig.
213 5B). These results demonstrate that transgenic wheat lines carrying RNAi
214 constructs can produce and process siRNA molecules which efficiently
215 down-regulate *PsFUZ7* in *Pst*, and also affect the expression of some related
216 genes in *Pst* and wheat.

217

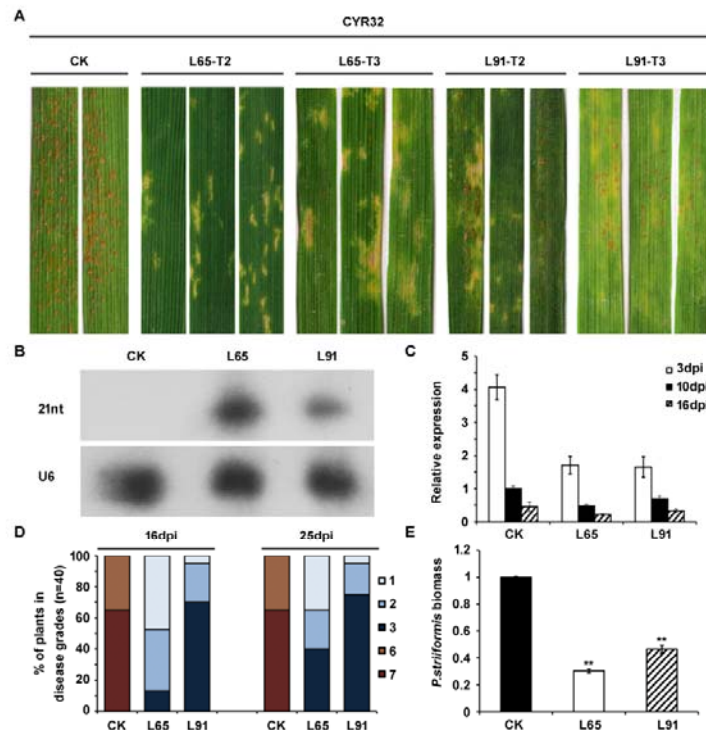


Figure 4. Transgenic wheat lines L65 and L91 producing fungal gene-derived siRNAs induce silencing of the target mRNA and confer resistance to *Pst* infection. A, Phenotypes of transgenic lines L65, L91, and control (CK) in T_2 and T_3 generations. The second leaves of seedlings were inoculated with urediospores of CYR32 and photographed at 14 dpi with *Pst* in each generation. CK, transgenic lines carrying empty vector; L65 and L91, transgenic lines carrying RNAi constructs. B, Northern blot analysis of siRNA isolated from T_3 transgenic wheat lines detected with specific probe derived from the *PsFUZ7* fragment. U6 small nuclear RNA as a loading control. C, Relative expression of *PsFUZ7* at 3, 10 and 16 dpi with CYR32 of T_3 transgenic wheat lines L65, L91, and control (CK). Data were normalized to *PsEF-1*, and the CK-10d control was set to 1. D, Host response and infection types in T_3 transgenic wheat lines L65, L91, and control (CK) assessed at 16 and 25 dpi with CYR32. E, Fungal biomass measured using real-time PCR of total DNA extracted from wheat leaves infected with CYR32 at 14 dpi. Ratio of total fungal DNA to total wheat DNA was assessed using the wheat gene *TaEF-1* and the *Pst* gene *PsEF-1*. Differences were assessed using Student's t-tests. Values represent the means \pm standard errors of three independent samples. Double asterisks indicate $P < 0.01$.

218 ***Pst* Development and Growth is Severely Suppressed in Transgenic** 219 **Wheat Lines Carrying *PsFUZ7* RNAi Constructs**

220 To investigate *Pst* development in transgenic wheat lines L65 and L91,
 221 fungal structures were stained with Wheat Germ Agglutinin (WGA) for
 222 microscopic observation. *Pst* in transgenic lines L65 and L91 exhibits poorly
 223 developed hyphae with minimal haustorium formation, while a widespread
 224 hyphal network with numerous haustoria in mesophyll cells is observed in
 225 control plants at 10 dpi with CYR32 (Fig. 6A-C). Notably, large areas of
 226 hypersensitive cell death are induced in transgenic lines L65 and L91 (Fig. 6A
 227 and D). The observed restriction of fungal development within

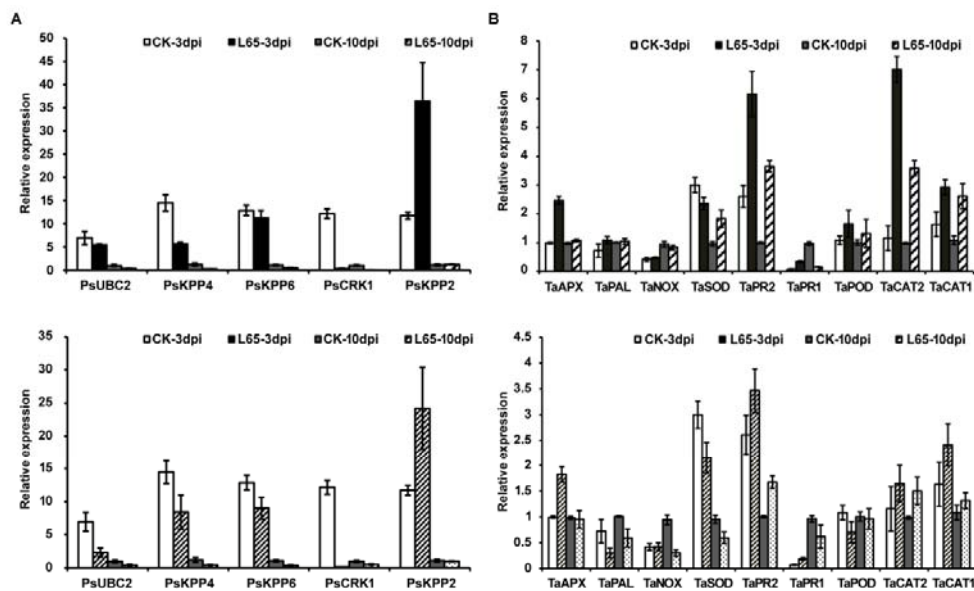


Figure 5. Transcript profiles of genes involved in the MAPK pathway in *Pst* and defense-related genes in transgenic wheat plants L65 and L91. (A) Transcript abundance of MAPK-pathway related genes in *Pst* decreases except for *PsKPP2*. Wheat leaves were sampled at 3 and 10 dpi with *Pst*. Data were normalized to the *PsEF-1* expression level, and the CK-10d control was set to 1. *PsKPP4*, MAP kinase kinase kinase; *PsFUZ7*, MAP kinase kinase; *PsKPP2*, *PsKPP6* and *PsCRK1*, MAP kinase. (B) Transcript abundance of pathogenesis-related proteins or defense-related genes increase in transgenic wheat plants L65 and L91 at 3 and 10 dpi. *TaPR1*, pathogenesis-related protein 1; *TaPR2*, β -1,3-glucanase; *TaPAL*, phenylalanine ammonia lyase; *TaAPX*, ascorbate peroxidase; *TaNOX*, NADPH oxidase; *TaSOD*, superoxide dismutase; *TaPOD*, peroxidase; *TaCAT2*, catalase 2; *TaCAT1*, catalase 1. The data were normalized to the *TaEF-1* expression level, and the CK-10d control was set to 1. Values represent the means \pm standard errors of three independent samples.

228 siRNA-producing host tissue is consistent with the measured reduction of
 229 fungal biomass and uredia formation.

230 To further visualize mycelial growth in *Pst*-infected wheat tissue,
 231 transmission electron microscopy was used to examine fungal morphology
 232 and wheat cells (Fig. 6E). Disassembly of the nuclear envelope and shrinkage
 233 of protoplasts are observed in *Pst* cells during colonization of the tissue of
 234 transgenic plants L65 and L91 (Fig. 6E). In addition, plant plasma membranes
 235 were ruptured where they contacted *Pst* hyphae. By contrast, both fungal and
 236 host cells developed normally in control lines (Fig. 6E). These results indicate
 237 that RNAi molecules stably expressed in transgenic wheat plants are able to

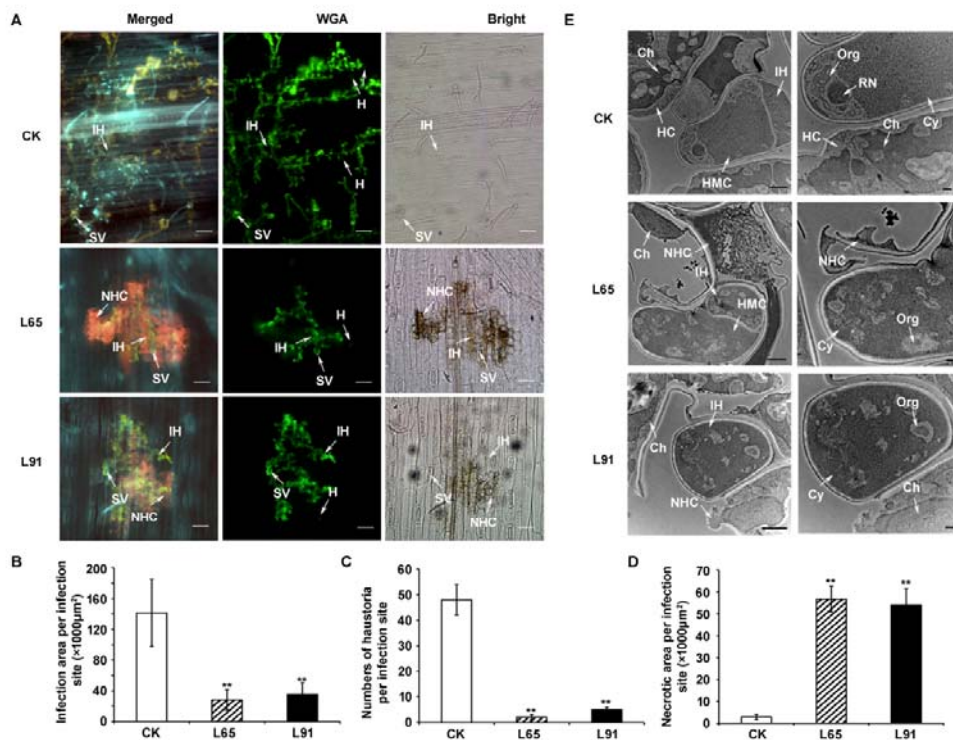


Figure 6. Microscopic visualization of the in host-induced gene silencing effect targeting *PsFUZ7* on colonization of wheat leaf tissue by *Pst*. A, Cytological observation of rust interaction with wheat by epifluorescence microscopy. Leaves inoculated with CYR32 were sampled at 10 dpi. SV, substomatal vesicle; IH, infection hypha; HMC, haustorial mother cell; H, haustorium; NHC, necrotic host cell. Bars = 50 μm . B, Infection area per infection site is reduced in the transgenic lines L65 and L91 infected with CYR32 compared with CK at 10 dpi. C, The formation of haustoria in lines L65 and L91 is inhibited after inoculation with CYR32 compared with CK at 10 dpi. D, The necrotic area of plants from lines L65 and L91 is increased compared with CK at 10 dpi with CYR32. E, Cytological observations of *Pst* CYR32 and wheat by transmission electron microscopy at 10 dpi. HMC, haustorial mother cell; H, haustorium; RN, rust nucleus; Ch, chloroplast; Cy, cytoplasm; IH, infection hypha; HC, host cell; NHC, necrotic host cell; Org, organelle. Left bars = 2 μm , Right bars = 500 nm. Differences in D-E were assessed using Student's t-tests. Values represent the means \pm standard errors of three independent samples. Double asterisks indicate $P < 0.01$.

238 confer genetically stable resistance to rust fungi by targeting fungal *PsFUZ7*

239 transcripts resulting in the suppression of *Pst* growth.

240

241

242 **DISCUSSION**

243 Currently, the most effective strategy to control stripe rust disease is the
244 application of fungicides. However, fungicide residues on food products remain
245 a threat to human health (Singh et al., 2015). Traditional plant breeding to
246 improve crop traits is another effective strategy but is time-consuming and
247 labor intensive (Saurabh et al., 2014). During the last two decades, research
248 efforts have focused on strategies to convert to biotechnological approaches
249 for crop improvement. The emergence of RNAi, which can be employed to
250 manipulate gene expression to improve quality traits in crops, offers potential
251 promise (Baulcombe, 2004; Saurabh et al., 2014). However, it remained
252 unclear whether *Pst* has a functional silencing system that can be induced in
253 transgenic wheat carrying RNAi constructs. Our approach was to determine
254 whether the expression of RNAi molecules derived from the MAPK kinase
255 gene *PsFUZ7* in transgenic wheat could confer genetically stable resistance to
256 rust pathogens of wheat. *PsFUZ7* was selected as the target gene for silencing
257 because it is expressed at high levels during penetration and parasitic stages
258 of the *Pst*-wheat interaction and showed the most positive phenotype in virus
259 induced transient silencing assays compared with two other kinases (Fig. 1). In
260 the fungal kingdom, MAPK kinases are evolutionarily conserved proteins that
261 function as key signal transduction components regulating a series of cellular
262 processes (Hamel et al., 2012). In the functional screening of candidate genes
263 for the generation of efficient RNAi sequences, supplementary assays
264 confirmed that the *PsFUZ7* is functionally conserved with MAPKKs from other
265 fungi and participates in development and morphogenesis critical for virulence
266 of *Pst*. Off-target effects, resulting in the knockdown of other transcripts with
267 limited similarity to siRNA, often occur during the application of RNAi in plants
268 and humans (Birmingham et al., 2006; De, 2014). In our study, no off-target
269 effects were detected, indicating that the *PsFUZ7* fragment selected to
270 generate RNAi constructs could be an ideal target for control of *Pst* via RNAi
271 (Supplemental Table S3).

272 The present study is devoted to illustrate an efficient alternative approach to
273 conventional breeding and fungicide treatment for fungal disease control. As
274 expected, transgenic lines carrying *PsFUZ7* RNAi constructs exhibit strong
275 and genetically stable resistance to *Pst* in T₃ generations (Fig. 4A). Generally,
276 the T₃ generation is considered the initial true transgenic line in hexaploid
277 wheat (Cheng et al., 2015a). Histological observations revealed differential
278 hyphal growth in transgenic lines carrying *PsFUZ7* RNAi constructs compared
279 to the control lines (Fig. 6). Previous studies demonstrated the efficient
280 transport of siRNA molecules from transgenic plant cells to the colonizing
281 pathogen (Nowara et al., 2010; Koch et al., 2013), and that the transported
282 siRNAs interfere with the target gene, affecting fungal growth through an
283 amplification of RNAi molecules and resulting in a resistance response
284 (Panwar et al., 2013; Cheng et al., 2015a). The suppression of *Pst* growth in
285 our study correlates with the production of siRNAs corresponding to the
286 targeted *PsFUZ7* sequences (Fig. 4B), as well as a significant reduction of
287 *PsFUZ7* transcripts and fungal biomass (Fig. 4C and E).

288 To explore the basis for the induction of necrosis in plant cells, a schematic
289 presentation for potential processes triggered by silencing *PsFUZ7* via the
290 expression of siRNA in transgenic wheat is presented (Fig. 7). In the plant
291 immunity system, two main phases, pathogen-associated molecular patterns
292 (PAMPs) triggered immunity (PTI) and effector-triggered immunity (ETI) are
293 well known (Jones and Dangl, 2006; Boller and Felix, 2009; Tsuda et al.,
294 2010). Cell death induced in transgenic wheat lines is in accordance with a
295 hypersensitive response (HR) that is expressed in pathogen specific ETI
296 (Jones and Dangl, 2006; Thomma et al., 2011). In *U. maydis*, the kinase CRK1
297 downstream of the MAPK cascade negatively regulates transcription and
298 secretion of some effector proteins (Bielska et al., 2014). In our study, we
299 verified the severe down-regulation of *PsCRK1* transcripts (Fig. 5) and the
300 interaction between *PsFUZ7* and *PsCRK1* via the yeast-two hybrid assay
301 (Supplemental Fig. S9). Considering these results, we propose that the

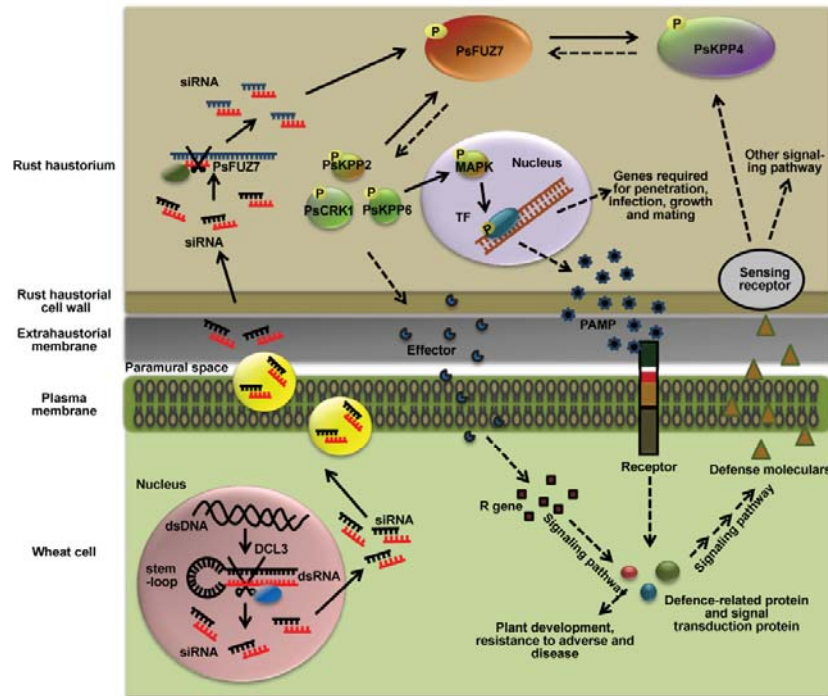


Figure 7. Schematic presentation of possible molecular dialogues between transgenic lines carrying RNAi constructs and colonizing *Pst*. Fungal dsRNA, produced inside transgenic wheat cells, is cleaved by the plant silencing machinery using endonuclease-type DICER enzymes into small silencing molecules (siRNAs). These siRNAs are trapped by a complex of proteins, and transported to the paramural space. After passing the haustorial cell wall, the silencing molecules trigger RNAi of their mRNA targets, and may act as primers leading to the activation of systemic silencing signals, thus inducing the immunity system of transgenic wheat by mechanisms including ETI and PTI.

302 expression of the siRNA target *PsFUZ7* influences effectors in *Pst* and triggers
 303 ETI in transgenic XN1376 wheat (Fig. 7). In addition, many features associated
 304 with fungal pathogenesis are dependent on signaling through MAPK
 305 cascades, including the biosynthesis, export, and secretion of different factors
 306 (Hamel et al., 2012). HIGS of *PsFUZ7* may impact biosynthesis or secretion of
 307 *Pst* components that may function as PAMPs in PTI (Chisholm et al., 2006).

308 Our study has confirmed that the expression of siRNA derived from a *Pst*
 309 pathogenicity gene in wheat is an effective strategy to control rust disease.
 310 This approach provides a huge reservoir of novel resources to enhance
 311 resistance to abiotic and biotic stress by the production of transgenic crops

312 that are environmentally friendly.

313

314 **MATERIALS AND METHODS**

315 **Fungi, Plants and Culture Conditions**

316 Chinese Yellow Rust isolate 32 (CYR32), which is a predominant race in
317 China (Wan et al., 2007), was used throughout this study. *Triticum aestivum* L.
318 cv. Suwon11 (Su11) that is susceptible to CYR32 was used in qRT-PCR and
319 VIGS assays. Plant cultivation and inoculation with *Pst* were performed as
320 described previously (Kang et al., 2002). XN1376, susceptible to CYR32 at the
321 seedling stage, was grown in an experimental field of Northwest A&F
322 University (Yangling, China) and used for transgenic wheat cultivars.

323 **VIGS and RNAi Vector Construction**

324 Two *PsFUZ7* fragments were used in BSMV-induced gene silencing
325 experiments (Supplemental Table S2). *PsFUZ7-1as* contains 218 bp of the
326 coding sequence from the 5' region, whereas *PsFUZ7-2as* encompasses
327 300-bp coding sequence in the 3' UTR. The two fragments were cloned into
328 BSMV as previously described (Holzberg et al., 2002). The hpRNA cassette
329 contains the *Zea mays* alcohol dehydrogenase 1 (*adh1*) gene as intron flanked
330 by the 300-bp fragment of *PsFUZ7* in sense and anti-sense orientation. The
331 expression cassette treated with *Sma*I and *Sac*I was cloned into the binary
332 vector pAHC25 using the same restriction sites (Christensen et al., 1992; Vasil
333 et al., 1993). The *bar* gene in the T-DNA of the vector as selection gene is
334 driven by the maize ubiquitin promoter, and the hpRNA cassette is also under
335 control of the Ubi promoter and terminated by the NOS terminator. The
336 resulting vectors were pAHC25-hp*PsFUZ7* for silencing *PsFUZ7*, and the
337 empty vector pAHC25 containing only the *bar* gene without a silencing
338 cassette.

339 **Total DNA, RNA Extraction, PCR and qRT-PCR**

340 Genomic DNA was extracted by the CTAB method (Porebski et al., 1997).
341 RNA was isolated with TRIZOL following the manufacturer's instructions
342 (Invitrogen, Carlsbad, CA, USA) and transcribed into cDNA also following the
343 manufacturer's directions (Promega, Madison, WI, USA). In each transgenic
344 generation, genomic DNA from leaves of transgenic wheat and control plants
345 were identified by PCR with two pairs of specific primers (TFUZ-F/R and
346 Bar-F/R, Supplemental Table S2) to detect the presence of the
347 sense-intron-antisense cassette in transgenic plants and the *bar* gene. To
348 measure fungal biomass, relative quantification of the single-copy target genes
349 in *PsEF-1* and *TaEF-1* (elongation factor-1) was carried out (Panwar et al.,
350 2013). Total genomic DNA of the wheat cultivar XN1376 or the *Pst* isolate
351 CYR32 was used to prepare standard curves derived from at least six serial
352 dilutions for each. The correlation coefficients for the analysis of the dilution
353 curves were above 0.99. The relative quantities of the PCR products of
354 *PsEF-1* and *TaEF-1* in mixed/infected samples were calculated using the
355 gene-specific standard curves to quantify the *Pst* and wheat genomic DNA,
356 respectively.

357 To measure the transcript levels of *PsFUZ7* by qRT-PCR, urediospores and
358 *in vivo* germ tubes of CYR32, plant tissue of Su11 infected with CYR32 at
359 6,12,18, 24, 36, 48, 72, 120, 168, 216 hours post inoculation (hpi) and
360 urediospores (US) were sampled. To analyze VIGS efficiency, qRT-PCR was
361 carried out 48 and 168 hpi with the CYR32 isolate. For transgenic efficiency
362 assay, total transgenic RNA for quantitative real-time PCR was extracted from
363 the second leaves of wheat at 3 dpi, 10 dpi, and 16 dpi with the CYR32 isolate.
364 All qRT-PCR was performed in a 20- μ L reaction mixture containing LightCycler
365 SYBR Green I Master Mix (Roche, Basel, Switzerland), 10 pmol each of the
366 forward and reverse gene-specific primers (Supplemental Table S2), and 2 μ L
367 of diluted cDNA (1:5) that was reverse transcribed. PCR was run in a
368 LightCycler 480II (Roche) under the conditions previously described (Cheng et
369 al., 2015b). Each sample was analyzed in three biological replications, and

370 each PCR analysis included three technical repeats. The data were
371 normalized to the *PsEF-1* expression level.

372

373 **BSMV-mediated Gene Silencing**

374 Capped *in vitro* transcripts were prepared from linearized plasmids
375 containing the tripartite BSMV genome (Petty et al., 1990) using the RiboMAX
376 TM Large-Scale RNA Production System-T7 and the Ribom7G Cap Analog
377 (Promega), according to the manufacturers' instructions. *PsFUZ7-1as* and
378 *PsFUZ7-2as* were used to inoculate wheat seedlings, while BSMV:*TaPDS*
379 (*TaPDS*: wheat phytoene desaturase gene) and BSMV: γ were used as
380 controls for the BSMV infection. Mock plants were inoculated with 1xFES
381 buffer as the negative control. Wheat seedlings with three leaves were used
382 for inoculation with BSMV, and BSMV-infected wheat plants were kept in a
383 growth chamber at $23 \pm 2^\circ\text{C}$. The fourth leaves were further inoculated with
384 fresh CYR32 urediospores at 10 d after virus inoculation, and the plants were
385 then maintained at $16 \pm 2^\circ\text{C}$ (Wang et al., 2007). The phenotypes of the fourth
386 leaves were recorded and photographed at 14 days after inoculation with *Pst*.
387 The number of uredia was counting a 1 cm^2 area at 14 dpi with *Pst* from at
388 least five randomly treated plants.

389 **Cytological Observation of Fungal Growth and Host Responses**

390 Leaf segments (1.5 cm long) were cut from inoculated leaves, fixed and
391 decolorized in ethanol/trichloromethane (3:1 v/v) containing 0.15% (w/v)
392 trichloroacetic acid for 3-5 days, and then treated as previously described
393 (Cheng et al., 2015b). To obtain high quality images of *Pst* infection structures
394 in wheat leaves, wheat germ agglutinin conjugated to Alexa-488 (Invitrogen)
395 was used as described (Ayliffe et al., 2011). Stained tissue was examined
396 under blue light excitation (excitation wavelength 450-480 nm, emission
397 wavelength 515 nm). Necrotic areas were observed via the auto-fl Stained t of
398 attacked mesophyll cells. Infection sites (30-50) from three leaves were

399 examined to record the number of haustorial mother cells, haustoria, hyphal
400 branches, hyphal length and infection areas of hyphae or necrotic area of host
401 cells in infected wheat per infection unit. The experiments were conducted in a
402 completely randomized block design with three replications. The presence of a
403 substomatal vesicle was defined as an established infection unit. Hyphal
404 length of *Pst* was measured from the substomatal vesicle to the apex of the
405 longest infection hypha. All microscopic observations were conducted with an
406 Olympus BX-51 microscope (Olympus, Tokyo, Japan).

407 To observe the ultrastructure of the fungus, wheat leaves bearing uredia
408 were cut into 0.5x0.5 cm pieces, immersed in 4% glutaraldehyde in 0.2 M
409 phosphate buffer, pH 6.8, and fixed at 4 °C overnight (Zhan et al., 2014). Fixed
410 leaf samples were washed four times with phosphate buffer for 15 min each.
411 Thereafter, samples were successively dehydrated for 30 min each in 30, 50,
412 70, 80 and 90% ethanol, and finally three times in 100% ethanol. The
413 dehydrated samples were treated with isoamyl acetate twice for 20 min each.
414 After drying in a CO₂ vacuum, the samples were sputter-coated with gold in an
415 E-1045 (Hitachi, Tokyo, Japan) and then examined with an S-4800 SEM
416 (Hitachi).

417 **Plant Transformation**

418 Immature embryos were isolated from spikes of XN1376 at 13-14 day post
419 anthesis in Yangling, Shaanxi. The isolated wheat embryos were cultured on
420 SD₂ medium in darks for 7-10 days for calli induction (Li et al., 2008). Then the
421 calli were moved to SD₂ medium added with 0.2 mol/l mannitol and 0.2 mol/l
422 sorbitol. After 4-6 hours, the calli were bombarded with 1-µm gold particles
423 coated with 1.5 µg of recombinant pAHC25 DNA using a PDS-1000 He biolistic
424 gun (BioRad, Hercules, CA, USA) at the pressure of 1,100 psi (Vasil et al.,
425 1993; Li et al., 2008). The bombarded calli were transferred onto osmotic
426 pressure medium described above for 16-18 h. Regeneration and selection
427 were carried out in the corresponding medium in the presence of 3-5 mg/l

428 bialaphos for the next few weeks, and the surviving plantlets with strong roots
429 and shoots were planted in a greenhouse in pots filled with soil (Cheng et al.,
430 2015a).

431

432 **Northern Blot**

433 About 30 µg of total RNA was subjected to electrophoresis on a denaturing
434 19% polyacrylamide gel, transferred to Nytran Super Charge Nylon
435 Membranes (Schleicher und Schuell MicroScience GmbH, Dassel, Germany)
436 and crosslinked using a Stratagene UV Crosslinker. The membranes were
437 prehybridized with PerfectHyb TM (Sigma-Aldrich, St. Louis, MO, USA), and
438 hybridized with the P³²-labeled DNA probes overnight in PerfectHyb buffer.
439 The membranes were autoradiographed on X-OMAT BT film (Carestream
440 Health, Rochester, NY, USA) after rinsing with washing buffer. U6 was used as
441 a loading control. The probe sequences are listed in Supplemental Table S2.

442

443 **FIGURE LEGENDS**

444 **Figure 1. Transcript profiles of five MAPK cascade genes at different**
445 ***Pst* infection stages.** Wheat leaves (Su11) were inoculated with fresh
446 urediospores (CYR32) and kept in the dark and under high humidity for 24 h.
447 Inoculated leaves were sampled at different time points according to the
448 differentiation stage of *Pst*. Gene expression levels were normalized to the
449 expression level of *PsEF-1*. Results are expressed as means ± standard errors
450 of three biological replicates. US: urediospores; 6 - 264 h: 6 - 264 hpi with
451 CYR32. *PsKPP4*: MAP kinase kinase kinase gene; *PsFUZ7*: MAP kinase
452 kinase gene; *PsKPP2*, *PsKPP6* and *PsCRK1*: MAP kinase genes.

453 **Figure 2. Functional assessment of *PsKPP4*, *PsFUZ7* and *PsKPP6* in**
454 **the wheat-*Pst* interaction by virus-induced gene silencing. A,** Phenotypes
455 of fourth leaves inoculated with CYR32 at 14 dpi. Plants were pre-inoculated

456 with FES buffer (mock), BSMV:*TaPDS*, BSMV: γ , BSMV:*PsKPP4-1as*,
457 BSMV:*PsKPP4-2as*, BSMV:*PsFUZ7-1as*, BSMV:*PsFUZ7-2as*,
458 BSMV:*PsKPP6-1as*, or BSMV:*PsKPP6-2as*, respectively. **B**, Relative
459 transcript levels of *PsKPP4*, *PsFUZ7* and *PsKPP6* in knockdown plants
460 inoculated with CYR32 at 2 and 7 dpi. Wheat leaves inoculated with BSMV: γ
461 and sampled after inoculation with CYR32 were used as controls. Data were
462 normalized to the transcript level of *PsEF-1*. Asterisks indicate $P < 0.05$,
463 double asterisks indicate $P < 0.01$. **C**, Quantification of uredial density in
464 silenced plants 14 dpi with CYR32. Differences were assessed using Student's
465 t-tests. Values represent the means \pm standard errors of three independent
466 samples. Asterisks indicate $P < 0.05$, double asterisks indicate $P < 0.01$.

467 **Figure 3. Epifluorescence observation of fungal growth in wheat**
468 **inoculated with BSMV and infected with CYR32.** Leaves inoculated with
469 CYR32 were sampled at 48 and 120 hpi and examined under an
470 epifluorescence microscope after staining with wheat germ agglutinin
471 conjugated to Alexa-488 (Invitrogen, Carlsbad, CA, USA). Treatments include
472 **A**, BSMV: γ ; **B**, BSMV:*PsFUZ7-1as* and **C**, BSMV:*PsFUZ7-2as* inoculated with
473 CYR32 at 48 hpi (Bars = 10 μm); **D**, BSMV: γ ; **E**, BSMV:*PsFUZ7-1as* and **F**,
474 BSMV:*PsFUZ7-2as* inoculated with CYR32 at 120 hpi (Bars = 50 μm). SV,
475 substomatal vesicle; HMC, haustorial mother cell; IH, infection hypha; H,
476 haustorium. **G**, Average number of haustoria (H), hyphal branches (HB) and
477 haustorial mother cells (HMC) in wheat inoculated with BSMV constructs and
478 infected with CYR32 at 48 hpi. **H**, Average length of infection hyphae (IH)
479 measured from their origin at the substomatal vesicle to the tip of the hypha in
480 wheat inoculated with BSMV constructs and infected with CYR32 at 48 hpi. **I**,
481 Infection area per infection site in wheat inoculated with BSMV and infected
482 with CYR32 at 120 hpi. Differences in **G-I** were assessed using Student's
483 t-tests. Values represent the means \pm standard errors of three independent
484 samples. Asterisks indicate $P < 0.05$, double asterisks indicate $P < 0.01$.

485 **Figure 4. Transgenic wheat lines L65 and L91 producing fungal**
486 **gene-derived siRNAs induce silencing of the target mRNA and confer**
487 **resistance to *Pst* infection. A**, Phenotypes of transgenic lines L65, L91, and
488 control (CK) in T₂ and T₃ generations. The second leaves of seedlings were
489 inoculated with urediospores of CYR32 and photographed at 14 dpi with *Pst* in
490 each generation. CK, transgenic lines carrying empty vector; L65 and L91,
491 transgenic lines carrying RNAi constructs. **B**, Northern blot analysis of siRNA
492 isolated from T₃ transgenic wheat lines detected with specific probe derived
493 from the *PsFUZ7* fragment. U6 small nuclear RNA as a loading control. **C**,
494 Relative expression of *PsFUZ7* at 3, 10, and 16 dpi with CYR32 of T₃
495 transgenic wheat lines L65, L91, and control (CK). Data were normalized to
496 *PsEF-1*, and the CK-10 d control was set to 1. **D**, Host response and infection
497 types in T₃ transgenic wheat lines L65, L91, and control (CK) assessed at 16
498 and 25 dpi with CYR32. **E**, Fungal biomass measured using real-time PCR of
499 total DNA extracted from wheat leaves infected with CYR32 at 14 dpi. Ratio of
500 total fungal DNA to total wheat DNA was assessed using the wheat gene
501 *TaEF-1* and the *Pst* gene *PsEF-1*. Differences were assessed using Student's
502 t-tests. Values represent the means ± standard errors of three independent
503 samples. Double asterisks indicate P < 0.01.

504 **Figure 5. Transcript profiles of genes involved in the MAPK pathway in**
505 ***Pst* and defense-related genes in transgenic wheat plants L65 and L91.**
506 (A) Transcript abundance of MAPK-pathway related genes in *Pst* decreases
507 except for *PsKPP2*. Wheat leaves were sampled at 3 and 10 dpi with *Pst*. Data
508 were normalized to the *PsEF-1* expression level, and the CK-10d control was
509 set to 1. *PsKPP4*, MAP kinase kinase kinase; *PsFUZ7*, MAP kinase kinase;
510 *PsKPP2*, *PsKPP6* and *PsCRK1*, MAP kinase. (B) Transcript abundance of
511 pathogenesis-related proteins or defense-related genes increase in transgenic
512 wheat plants L65 and L91 at 3 and 10 dpi. *TaPR1*, pathogenesis-related
513 protein 1; *TaPR2*, β-1,3-glucanase; *TaPAL*, phenylalanine ammonia lyase;

514 *TaAPX*, ascorbate peroxidase; *TaNOX*, NADPH oxidase; *TaSOD*, superoxide
515 dismutase; *TaPOD*, peroxidase; *TaCAT2*, catalase 2; *TaCAT1*, catalase 1. The
516 data were normalized to the *TaEF-1* expression level, and the CK-10d control
517 was set to 1. Values represent the means \pm standard errors of three
518 independent samples.

519 **Figure 6. Microscopic visualization of the in host-induced gene**
520 **silencing effect targeting *PsFUZ7* on colonization of wheat leaf tissue by**
521 ***Pst*. A,** Cytological observation of rust interaction with wheat by
522 epifluorescence microscopy. Leaves inoculated with CYR32 were sampled at
523 10 dpi. SV, substomatal vesicle; IH, infection hypha; HMC, haustorial mother
524 cell; H, haustorium; NHC, necrotic host cell. Bars = 50 μ m. **B,** Infection area
525 per infection site is reduced in the transgenic lines L65 and L 91 infected with
526 CYR32 compared with CK at 10 dpi. **C,** The formation of haustoria in lines L65
527 and L91 is inhibited after inoculation with CYR32 compared with CK at 10 dpi.
528 **D,** The necrotic area of plants from lines L65 and L91 is increased compared
529 with CK at 10 dpi with CYR32. **E,** Cytological observations of *Pst* CYR32 and
530 wheat by transmission electron microscopy at 10 dpi. HMC, haustorial mother
531 cell; H, haustorium; RN, rust nucleus; Ch, chloroplast; Cy, cytoplasm; IH,
532 infection hypha; HC, host cell; NHC, necrotic host cell; Org, organelle. Left
533 bars = 2 μ m, Right bars = 500 nm. Differences in **D-E** were assessed using
534 Student's t-tests. Values represent the means \pm standard errors of three
535 independent samples. Double asterisks indicate $P < 0.01$.

536 **Figure 7. Schematic presentation of possible molecular dialogues**
537 **between transgenic lines carrying RNAi constructs and colonizing *Pst*.**
538 Fungal dsRNA, produced inside transgenic wheat cells, is cleaved by the plant
539 silencing machinery using endonuclease-type DICER enzymes into small
540 silencing molecules (siRNAs). These siRNAs are trapped by a complex of
541 proteins, and transported to the paramural space. After passing the haustorial
542 cell wall, the silencing molecules trigger RNAi of their mRNA targets, and may

25

543 act as primers leading to the activation of systemic silencing signals, thus
544 inducing the immunity system of transgenic wheat by mechanisms including
545 ETI and PTI.

546

547 **SUPPLEMENTAL DATA**

548 **Supplemental Figure S1.** Relative transcript levels of (A) *PsKPP4*, (B)
549 *PsFUZ7*, and (C) *PsKPP6* homologs in respective knockdown plants
550 inoculated with CYR32 at 2 dpi.

551 **Supplemental Figure S2.** Multiple sequence alignment of *FUZ7* orthologs.

552 **Supplemental Figure S3.** Complementation of the *mst7* mutant of
553 *Magnaporthe oryzae* with *PsFUZ7*.

554 **Supplemental Figure S4.** Overexpression assay of *PsFUZ7* in the fission
555 yeast SP-Q01.

556 **Supplemental Figure S5.** Effect of the immuno-suppressive inhibitor U0126
557 on germination of *Pst*.

558 **Supplemental Figure S6.** Structure of the pAHC25-*PsFUZ7* RNAi construct
559 and molecular identification in transgenic plants.

560 **Supplemental Figure S7.** Transcript abundance of putative off-target in *Pst*
561 after L65, L91 and CK inoculated with CYR32 at 10dpi.

562 **Supplemental Figure S8.** Transcript abundance of putative off-target in wheat
563 after L65, L91 and CK inoculated with CYR32 at 10dpi.

564 **Supplemental Figure S9.** Y2H assay using MAPK cascade genes.

565 **Supplemental Table S1.** MAPK orthologs identified in *Pst*.

566 **Supplemental Table S2.** Primers used in this study.

567 **Supplemental Table S3.** Homologs of PsKPP4, PsFUZ7 and PsKPP6 in *Pst*.

568 **Supplemental Table S4.** Prediction of *PsFUZ7* off-target transcripts.

569

570

571 **ACKNOWLEDGMENTS**

572 The authors thank Professor Jiankang Zhu from Shanghai Center for Plant
573 Stress Biology, SIBS, CAS, China for providing technical supports on
574 Southern blot and Northern blot, and Professor Larry Dunkle from the
575 USDA-Agricultural Research Service at Purdue University, USA for critical
576 reading the manuscript.

577

578

Parsed Citations

Ayliffe M, Devilla R, Mago R, White R, Talbot M, Pryor A, Leung H (2011) Nonhost resistance of rice to rust pathogens. Mol Plant Microbe Interact 24: 1143-1155

Pubmed: [Author and Title](#)
CrossRef: [Author and Title](#)
Google Scholar: [Author Only](#) [Title Only](#) [Author and Title](#)

Bartel DP (2004) MicroRNAs: genomics, biogenesis, mechanism, and function. Cell 116: 281-297

Pubmed: [Author and Title](#)
CrossRef: [Author and Title](#)
Google Scholar: [Author Only](#) [Title Only](#) [Author and Title](#)

Baulcombe D (2004) RNA silencing in plants. Nature 431: 356-363

Pubmed: [Author and Title](#)
CrossRef: [Author and Title](#)
Google Scholar: [Author Only](#) [Title Only](#) [Author and Title](#)

Baum JA, Bogaert T, Clinton W, Heck GR, Feldmann P, Ilagan O, Johnson S, Plaetinck G, Munyikwa T, Pleau M (2007) Control of coleopteran insect pests through RNA interference. Nat Biotechnol 25: 1322-1326

Pubmed: [Author and Title](#)
CrossRef: [Author and Title](#)
Google Scholar: [Author Only](#) [Title Only](#) [Author and Title](#)

Bielska E, Higuchi Y, Schuster M, Steinberg N, Kilaru S, Talbot NJ, Steinberg G (2014) Long-distance endosome trafficking drives fungal effector production during plant infection. Nat Commun 5: 5097

Pubmed: [Author and Title](#)
CrossRef: [Author and Title](#)
Google Scholar: [Author Only](#) [Title Only](#) [Author and Title](#)

Birmingham A, Anderson EM, Reynolds A, Ilsleytree D, Leake D, Fedorov Y, Baskerville S, Maksimova E, Robinson K, Karpilow J (2006) 3' UTR seed matches, but not overall identity, are associated with RNAi off-targets. Nat Methods 3: 199-204

Pubmed: [Author and Title](#)
CrossRef: [Author and Title](#)
Google Scholar: [Author Only](#) [Title Only](#) [Author and Title](#)

Boller T, Felix G (2009) A renaissance of elicitors: perception of Microbe-Associated Molecular Patterns and danger signals by Pattern-Recognition Receptors. Plant Biol 60: 379-406

Pubmed: [Author and Title](#)
CrossRef: [Author and Title](#)
Google Scholar: [Author Only](#) [Title Only](#) [Author and Title](#)

Chen T, Zhu H, Ke D, Cai K, Wang C, Gou H, Hong Z, Zhang Z (2012) A MAP kinase kinase interacts with SymRK and regulates nodule organogenesis in Lotus japonicus. Plant Cell 24: 823-838

Pubmed: [Author and Title](#)
CrossRef: [Author and Title](#)
Google Scholar: [Author Only](#) [Title Only](#) [Author and Title](#)

Chen WQ, Wu LR, Liu TG, Xu SC, Jin SL, Peng YL, Wang BT (2009) Race dynamics, diversity, and virulence evolution in Puccinia striiformis f. sp. tritici, the causal agent of wheat stripe rust in China from 2003 to 2007. Plant Dis 93: 1093-1101

Pubmed: [Author and Title](#)
CrossRef: [Author and Title](#)
Google Scholar: [Author Only](#) [Title Only](#) [Author and Title](#)

Chen XM (2014) Integration of cultivar resistance and fungicide application for control of wheat stripe rust. Can J Plant Pathol 36: 311-326

Pubmed: [Author and Title](#)
CrossRef: [Author and Title](#)
Google Scholar: [Author Only](#) [Title Only](#) [Author and Title](#)

Cheng W, Song XS, Li HP, Cao LH, Sun K, Qiu XL, Xu YB, Yang P, Huang T, Zhang JB (2015a) Host-induced gene silencing of an essential chitin synthase gene confers durable resistance to Fusarium head blight and seedling blight in wheat. Plant Biotechnol J 13: 1335-1345

Pubmed: [Author and Title](#)
CrossRef: [Author and Title](#)
Google Scholar: [Author Only](#) [Title Only](#) [Author and Title](#)

Cheng Y, Wang X, Yao J, Voegelé RT, Zhang Y, Wang W, Huang L, Kang Z (2015b) Characterization of protein kinase PsSRPKL, a novel pathogenicity factor in the wheat stripe rust fungus. Environ Microbiol 17: 2601-2617

Pubmed: [Author and Title](#)
CrossRef: [Author and Title](#)
Google Scholar: [Author Only](#) [Title Only](#) [Author and Title](#)

Chisholm ST, Coaker G, Day B, Staskawicz BJ (2006) Host-microbe interactions: shaping the evolution of the plant immune response.

Cell 124: 803-814

Pubmed: [Author and Title](#)
CrossRef: [Author and Title](#)
Google Scholar: [Author Only Title Only Author and Title](#)

Christensen AH, Sharrock RA, Quail PH (1992) Maize polyubiquitin genes: structure, thermal perturbation of expression and transcript splicing, and promoter activity following transfer to protoplasts by electroporation. Plant Mol Biol 18: 675-689

Pubmed: [Author and Title](#)
CrossRef: [Author and Title](#)
Google Scholar: [Author Only Title Only Author and Title](#)

De SN (2014) Off-targets in RNAi screens. Nat Methods 11: 480

Pubmed: [Author and Title](#)
CrossRef: [Author and Title](#)
Google Scholar: [Author Only Title Only Author and Title](#)

Fagard M, Boutet S, Morel JB, Bellini C, Vaucheret H (2000) AGO1, QDE-2, and RDE-1 are related proteins required for post-transcriptional gene silencing in plants, quelling in fungi, and RNA interference in animals. Proc Natl Acad Sci USA 97: 11650-11654

Pubmed: [Author and Title](#)
CrossRef: [Author and Title](#)
Google Scholar: [Author Only Title Only Author and Title](#)

Fu Y, Duan X, Tang C, Li X, Voegelé RT, Wang X, Wei G, Kang Z (2014) TaADF7, an actin-depolymerizing factor, contributes to wheat resistance against *Puccinia striiformis* f. sp. tritici. Plant J 78: 16-30

Pubmed: [Author and Title](#)
CrossRef: [Author and Title](#)
Google Scholar: [Author Only Title Only Author and Title](#)

Ghag SB, Shekhawat UK, Ganapathi TR (2014) Host-induced post-transcriptional hairpin RNA-mediated gene silencing of vital fungal genes confers efficient resistance against *Fusarium wilt* in banana. Plant Biotechnol J 12: 541-553

Pubmed: [Author and Title](#)
CrossRef: [Author and Title](#)
Google Scholar: [Author Only Title Only Author and Title](#)

Ghildiyal M, Zamore PD (2009) Small silencing RNAs: an expanding universe. Nat Rev Genet 10: 94-108

Pubmed: [Author and Title](#)
CrossRef: [Author and Title](#)
Google Scholar: [Author Only Title Only Author and Title](#)

Hamal A, Jouannic S, Leprince AS, Kreis M, Henry Y (1999) Molecular characterisation and expression of an *Arabidopsis thaliana* L. MAP kinase kinase cDNA, AtMAP2Ka. Plant Sci 140: 41-52

Pubmed: [Author and Title](#)
CrossRef: [Author and Title](#)
Google Scholar: [Author Only Title Only Author and Title](#)

Hamel LP, Nicole MC, Duplessis S, Ellis BE (2012) Mitogen-activated protein kinase signaling in plant-interacting fungi: distinct messages from conserved messengers. Plant Cell 24: 1327-1351

Pubmed: [Author and Title](#)
CrossRef: [Author and Title](#)
Google Scholar: [Author Only Title Only Author and Title](#)

Holzberg S, Brosio P, Gross C, Pogue GP (2002) Barley stripe mosaic virus-induced gene silencing in a monocot plant. Plant J 30: 315-327

Pubmed: [Author and Title](#)
CrossRef: [Author and Title](#)
Google Scholar: [Author Only Title Only Author and Title](#)

Huang G, Allen R, Davis EL, Baum TJ, Hussey RS (2006) Engineering broad root-knot resistance in transgenic plants by RNAi silencing of a conserved and essential root-knot nematode parasitism gene. Proc Natl Acad Sci USA 103: 14302-14306

Pubmed: [Author and Title](#)
CrossRef: [Author and Title](#)
Google Scholar: [Author Only Title Only Author and Title](#)

Ishii H (2006) Impact of fungicide resistance in plant pathogens on crop disease control and agricultural environment. Jpn Ag R RES Q 40: 205-211

Pubmed: [Author and Title](#)
CrossRef: [Author and Title](#)
Google Scholar: [Author Only Title Only Author and Title](#)

Jones JD, Dangl JL (2006) The plant immune system. Nature 444: 323-329

Pubmed: [Author and Title](#)
CrossRef: [Author and Title](#)
Google Scholar: [Author Only Title Only Author and Title](#)

Kang Z, Huang L, Buchenauer H (2002) Ultrastructural changes and localization of lignin and callose in compatible and incompatible interactions between wheat and *Puccinia striiformis*. J Plant Dis Protect 109: 25-37

Pubmed: [Author and Title](#)
CrossRef: [Author and Title](#)
Google Scholar: [Author Only](#) [Title Only](#) [Author and Title](#)

Koch A, Kumar N, Weber L, Keller H, Imani J, Kogel KH (2013) Host-induced gene silencing of cytochrome P450 lanosterol C14 α -demethylase-encoding genes confers strong resistance to Fusarium species. Proc Natl Acad Sci USA 110: 19324-19329

Pubmed: [Author and Title](#)
CrossRef: [Author and Title](#)
Google Scholar: [Author Only](#) [Title Only](#) [Author and Title](#)

Li HP, Zhang JB, Shi RP, Huang T, Fischer R, Liao YC (2008) Engineering Fusarium head blight resistance in wheat by expression of a fusion protein containing a Fusarium-specific antibody and an antifungal peptide. Mol Plant Microbe Interact 21: 1242-1248

Pubmed: [Author and Title](#)
CrossRef: [Author and Title](#)
Google Scholar: [Author Only](#) [Title Only](#) [Author and Title](#)

Liu QH (2010) Biochemical principles of small RNA pathways. Annu Rev Biochem 79: 295-319

Pubmed: [Author and Title](#)
CrossRef: [Author and Title](#)
Google Scholar: [Author Only](#) [Title Only](#) [Author and Title](#)

Mao YB, Cai WJ, Wang JW, Hong GJ, Tao XY, Wang LJ, Huang YP, Chen XY (2007) Silencing a cotton bollworm P450 monooxygenase gene by plant-mediated RNAi impairs larval tolerance of gossypol. Nat Biotechnol 25: 1307-1313

Pubmed: [Author and Title](#)
CrossRef: [Author and Title](#)
Google Scholar: [Author Only](#) [Title Only](#) [Author and Title](#)

Mcintosh RA, Wellings CR, Park RF (1995) Wheat rusts: an atlas of resistance genes. Csiro Publishing, East Melbourne

Pubmed: [Author and Title](#)
CrossRef: [Author and Title](#)
Google Scholar: [Author Only](#) [Title Only](#) [Author and Title](#)

McNeal F, Konzak C, Smith E, Tate W, Russell T (1971) A uniform system for recording and processing cereal research data. USDA Bulletin, ARS, 34-121, pp. 42

Pubmed: [Author and Title](#)
CrossRef: [Author and Title](#)
Google Scholar: [Author Only](#) [Title Only](#) [Author and Title](#)

Nowara D, Gay A, Lacomme C, Shaw J, Ridout C, Douchkov D, Hensel G, Kumlehn J, Schweizer P (2010) HIGS: host-induced gene silencing in the obligate biotrophic fungal pathogen Blumeria graminis. Plant Cell 22: 3130-3141

Pubmed: [Author and Title](#)
CrossRef: [Author and Title](#)
Google Scholar: [Author Only](#) [Title Only](#) [Author and Title](#)

Panwar V, Mccallum B, Bakkeren G (2013) Endogenous silencing of Puccinia triticina pathogenicity genes through in planta-expressed sequences leads to the suppression of rust diseases on wheat. Plant J 73: 521-532

Pubmed: [Author and Title](#)
CrossRef: [Author and Title](#)
Google Scholar: [Author Only](#) [Title Only](#) [Author and Title](#)

Petty ITD, French R, Jones RW, Jackson AO (1990) Identification of barley stripe mosaic virus genes involved in viral RNA replication and systemic movement. EMBO J 9: 3453-3457

Pubmed: [Author and Title](#)
CrossRef: [Author and Title](#)
Google Scholar: [Author Only](#) [Title Only](#) [Author and Title](#)

Porebski S, Bailey LG, Baum BR (1997) Modification of a CTAB DNA extraction protocol for plants containing high polysaccharide and polyphenol components. Plant Mol Biol Rep 15: 8-15

Pubmed: [Author and Title](#)
CrossRef: [Author and Title](#)
Google Scholar: [Author Only](#) [Title Only](#) [Author and Title](#)

Saurabh S, Vidyarthi AS, Prasad D (2014) RNA interference: concept to reality in crop improvement. Planta 239: 543-564

Pubmed: [Author and Title](#)
CrossRef: [Author and Title](#)
Google Scholar: [Author Only](#) [Title Only](#) [Author and Title](#)

Scofield SR, Huang L, Brandt AS, Gill BS (2005) Development of a virus-induced gene-silencing system for hexaploid wheat and its use in functional analysis of the Lr21-mediated leaf rust resistance pathway. Plant Physiol 138: 2165-2173

Pubmed: [Author and Title](#)
CrossRef: [Author and Title](#)
Google Scholar: [Author Only](#) [Title Only](#) [Author and Title](#)

Singh RP, Hodson DP, Huertaespino J, Jin Y, Bhavani S, Njau P, Herrerafoessel S, Singh PK, Singh S, Govindan V (2011) The emergence of Ug99 races of the stem rust fungus is a threat to world wheat production. Ann Rev Phytopathol 49: 465-481

Pubmed: [Author and Title](#)
Downloaded from on November 5, 2017 - Published by www.plantphysiol.org
Copyright © 2017 American Society of Plant Biologists. All rights reserved.

CrossRef: [Author and Title](#)
Google Scholar: [Author Only](#) [Title Only](#) [Author and Title](#)

Singh RP, Hodson DP, Jin Y, Lagudah ES, Ayliffe MA, Bhavani S, Rouse MN, Pretorius ZA, Szabo LJ, Huerta-Espino J (2015) Emergence and spread of new races of wheat stem rust fungus: continued threat to food security and prospects of genetic control. *Phytopathology* 105: 872-884

Pubmed: [Author and Title](#)
CrossRef: [Author and Title](#)
Google Scholar: [Author Only](#) [Title Only](#) [Author and Title](#)

Thomma BPHJ, Nürnberger T, Joosten MHAJ (2011) Of PAMPs and effectors: the blurred PTI-ETI dichotomy. *Plant Cell* 23: 4-15

Pubmed: [Author and Title](#)
CrossRef: [Author and Title](#)
Google Scholar: [Author Only](#) [Title Only](#) [Author and Title](#)

Tsuda K, Katagiri F, Parker JE, Ellis JG (2010) Comparing signaling mechanisms engaged in pattern-triggered and effector-triggered immunity. *Curr Opin Plant Biol* 13: 459-465

Pubmed: [Author and Title](#)
CrossRef: [Author and Title](#)
Google Scholar: [Author Only](#) [Title Only](#) [Author and Title](#)

Van Drogen F, Peter M (2002) MAP Kinase cascades: scaffolding signal specificity. *Curr Biol* 12: R53-R55

Pubmed: [Author and Title](#)
CrossRef: [Author and Title](#)
Google Scholar: [Author Only](#) [Title Only](#) [Author and Title](#)

Vasil V, Srivastava V, Castillo AM, Fromm ME, Vasil IK (1993) Rapid production of transgenic wheat plants by direct bombardment of cultured immature embryos. *Nat Biotechnol* 11: 1553-1558

Pubmed: [Author and Title](#)
CrossRef: [Author and Title](#)
Google Scholar: [Author Only](#) [Title Only](#) [Author and Title](#)

Wan AM, Chen XM, He ZH (2007) Wheat stripe rust in China. *Crop Pasture Sci* 58: 605-619

Pubmed: [Author and Title](#)
CrossRef: [Author and Title](#)
Google Scholar: [Author Only](#) [Title Only](#) [Author and Title](#)

Wang CF, Huang LL, Buchenauer H, Han QM, Zhang HC, Kang ZS (2007) Histochemical studies on the accumulation of reactive oxygen species (O₂- and H₂O₂) in the incompatible and compatible interaction of wheat-Puccinia striiformis f. sp. tritici. *Physiol Mol Plant Pathol* 71: 230-239

Pubmed: [Author and Title](#)
CrossRef: [Author and Title](#)
Google Scholar: [Author Only](#) [Title Only](#) [Author and Title](#)

Wellings CR (2011) Global status of stripe rust: a review of historical and current threats. *Euphytica* 179: 129-141

Pubmed: [Author and Title](#)
CrossRef: [Author and Title](#)
Google Scholar: [Author Only](#) [Title Only](#) [Author and Title](#)

Yin CT, Jurgenson J E, Hulbert S H (2011) Development of a host-induced RNAi system in the wheat stripe rust fungus *Puccinia striiformis* f. sp. tritici. *Mol Plant Microbe Interact* 24: 554-561

Pubmed: [Author and Title](#)
CrossRef: [Author and Title](#)
Google Scholar: [Author Only](#) [Title Only](#) [Author and Title](#)

Zhan G, Tian Y, Wang F, Chen X, Guo J, Jiao M, Huang L, Kang Z (2014) A novel fungal hyperparasite of *Puccinia striiformis* f. sp. tritici, the causal agent of wheat stripe rust. *PLoS ONE* 9: e111484

Pubmed: [Author and Title](#)
CrossRef: [Author and Title](#)
Google Scholar: [Author Only](#) [Title Only](#) [Author and Title](#)